

Magnetic resonance hybridization and optical activity of microwaves in a chiral metamaterial

T. Q. Li, H. Liu, T. Li, S. M. Wang, F. M. Wang, R. X. Wu, P. Chen, S. N. Zhu, and X. Zhang

Citation: [Applied Physics Letters](#) **92**, 131111 (2008); doi: 10.1063/1.2905285

View online: <http://dx.doi.org/10.1063/1.2905285>

View Table of Contents: <http://scitation.aip.org/content/aip/journal/apl/92/13?ver=pdfcov>

Published by the [AIP Publishing](#)

Articles you may be interested in

[Complementary chiral metamaterials with giant optical activity and negative refractive index](#)

Appl. Phys. Lett. **98**, 161907 (2011); 10.1063/1.3574909

[90° polarization rotator using a bilayered chiral metamaterial with giant optical activity](#)

Appl. Phys. Lett. **96**, 203501 (2010); 10.1063/1.3429683

[Microwave transmissivity of a metamaterial–dielectric stack](#)

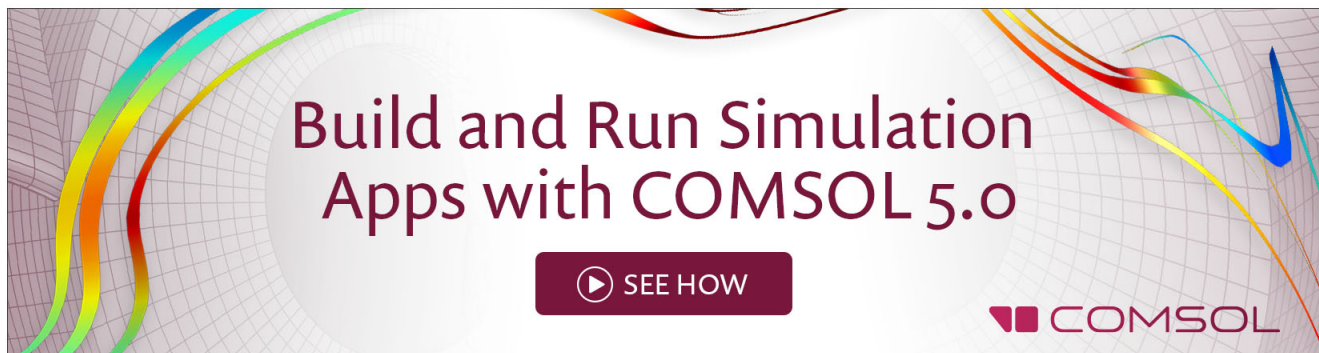
Appl. Phys. Lett. **95**, 174101 (2009); 10.1063/1.3253703

[Optical activity in extrinsically chiral metamaterial](#)

Appl. Phys. Lett. **93**, 191911 (2008); 10.1063/1.3021082

[Strong optical activity in chiral metamaterials of metal screw hole arrays](#)

Appl. Phys. Lett. **89**, 211105 (2006); 10.1063/1.2392787

A promotional banner for COMSOL 5.0. It features a background of a grid with colorful, flowing lines in shades of blue, green, yellow, and red. The text 'Build and Run Simulation Apps with COMSOL 5.0' is centered in a dark red font. Below the text is a dark red button with a white play icon and the text 'SEE HOW'. The COMSOL logo is in the bottom right corner.

Magnetic resonance hybridization and optical activity of microwaves in a chiral metamaterial

T. Q. Li,¹ H. Liu,^{1,a)} T. Li,¹ S. M. Wang,¹ F. M. Wang,¹ R. X. Wu,² P. Chen,² S. N. Zhu,^{1,a)} and X. Zhang³

¹Department of Physics, National Laboratory of Solid State Microstructures, Nanjing University, Nanjing 210093, People's Republic of China

²Department of Electronic Sciences and Engineering, Key Laboratory of Modern Acoustics, Nanjing University, Nanjing 210093, People's Republic of China

³5130 Etcheverry Hall, Nanoscale Science and Engineering Center, University of California, Berkeley, California 94720-1740, USA

(Received 29 January 2008; accepted 14 March 2008; published online 2 April 2008)

The propagation of microwaves through a chiral metamaterial based on a magnetic dimer is experimentally studied. As proposed by our previous theoretical model, two resonance peaks are obtained in the transmission spectrum; these originate from the hybridization effect of magnetic resonance modes in this system. Optical activity is also observed in the transmission wave. The polarization state dramatically changes around the resonance frequency: the transmitted wave becomes elliptically polarized with its major polarization axis approximately perpendicular to that of the linear incident wave. This coupled magnetic dimer system provides a practical method to optically design tunable active medium and device. © 2008 American Institute of Physics.

[DOI: 10.1063/1.2905285]

In 1999,¹ Pendry *et al.* reported that a nonmagnetic metallic element—a double split-ring resonator (DSRR)—sized below the diffraction limit exhibits strong magnetic responses and behaves like an effective negative permeability material. Despite the absence of free magnetic poles in such systems, the excitation of displacement currents in the DSRR results in the induction of a magnetic dipole moment that is somewhat similar to a bar magnet. Analogous to the surface plasmon resonance in metal nanoparticles, an effective medium made of DSRRs could support resonant magnetic plasmon (MP) oscillations at gigahertz^{1–4} and terahertz frequencies and within the visible spectral region.^{4–12} Combined with an electric response and characterized by negative permittivity, such systems could lead to the development of metamaterials with negative indexes of refraction.^{2,3}

On the other hand, however, it was also suggested that a combination of magnetic response and chirality could be used as an alternative route to negative refraction.¹³ Further, various electromagnetic chiral structures have been reported in the microwave spectral range, such as helical wire spring,¹⁴ swiss-rod metal structure,¹³ rotating rosette shape,^{15,16} and H-shape.¹⁷ In our recent paper,¹⁸ we proposed a theoretical model to show that the coupling effect between two split-ring resonators can be used to produce optical activity and the rotation of polarization can be tuned by changing the coupling strength.

In this paper, we present the first experimental verification of the results proposed by the theoretical model described in Ref. 18. We design and experimentally investigate an array of magnetic dimers (MDs) that are made of two square single split-ring resonators (SSRRs). Further, we focus on the polarization property: an incident wave of linear polarization changes its polarization state when passing through this coupled system. This optical activity is caused

by the coupling of the SSRRs and is not observed in the individual SSRR.

Figure 1(a) shows the basic element of the MD and all its characteristic sizes—it comprises two square copper rings with their slits perpendicular to each other—the slit of the first SSRR is parallel to the x axis and that of the second is along the y axis. These two rings are separated by a distance D that is filled with polystyrene (of which the permittivity is 4). Our array comprises these MDs positioned in the x - y plane and the lattice period is set at 4.64 mm.

In the experimental setup [see Fig. 1(b)], a linearly polarized microwave with \vec{E} field along the y direction extends from the source and perpendicularly passes through the plan of our MD array. A detector (Agilent E8363A vector network analyzer) is set on the other side of the plan to receive the transmitted signal; it records the amplitude and phase of both the x and y components of the transmitted wave. Further, the frequency range of the electromagnetic wave is set below 20 GHz based on the measurement capacity of the detector.

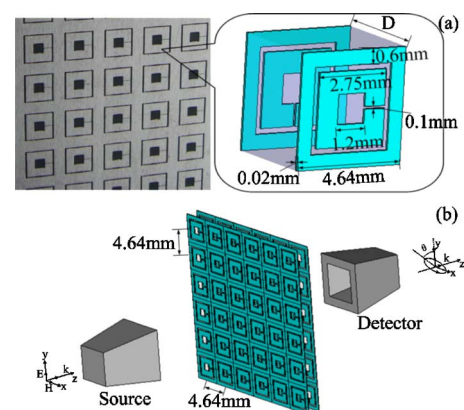


FIG. 1. (Color online) (a) Photograph of magnetic dimers (inset: structure of one unit cell). (b) Schematic picture of the experimental setup, the incident wave is emitted from the source (on the left) and is received by the detector (on the right), the polarization direction of the incident wave is along the y axis.

^{a)}Authors to whom correspondence should be addressed. Electronic addresses: liuhuiemail@yahoo.com and zhushn@nju.edu.cn.

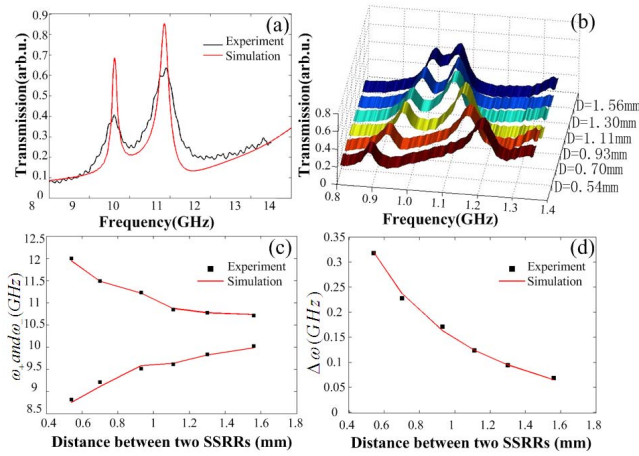


FIG. 2. (Color online) (a) The amplitude of transmitted wave through the array of magnetic dimers with $D=1.11$ mm, experiment result (black line) and simulation result [gray (red) line]. (b) Transmission results under the different D . (c) Resonance frequencies on the distance D . (d) Frequency gap $\Delta\omega=\omega_2-\omega_1$ on the distance D .

Figure 2(a) (black line) shows the experimental result of transmission under $D=1.11$ mm. We observe two obvious resonance peaks in the transmission curve that correspond to the two excited magnetic resonant modes anticipated in our theoretical model.¹⁸ In order to compare and examine the experimental result, we employ finite-difference time-domain simulation by using a commercial software package—CST MICROWAVE STUDIO. The simulated transmission result is also shown in Fig. 2(a) (red line); it is observed that the simulated and experimental results are in good agreement. Then, we tune the thickness of the middle layer between the two SSRRs with six discrete values ranging from 0.54 to 1.56 mm; the measured transmission results for each distance are shown in Fig. 2(b). As the distance D increases, the two resonance peaks gradually join each other with the blurring of their bounds [see Fig. 2(b)], and the frequency gap between the two resonance peaks accordingly decreases [see Figs. 2(c) and 2(d)].

In order to explain the two resonance peaks described above, here, we introduce Lagrangian formalism to describe the MD. We begin from the single SSRR, and then expand it to the coupled condition of our system. One SSRR can be viewed as an ideal LC circuit—the metal ring is regarded as a magnetic loop with inductance L and the slit of the ring is a capacitor with capacitance C . Thus, this system has a resonance frequency of $\omega_0=1/\sqrt{LC}$, and the oscillating current induced in the resonator generates the magnetic moment. If we define the charge accumulated in the slit as a generalized coordinate, the Lagrangian of SSRR can be written in a rather simple form: $\Gamma=L\dot{Q}^2/2-Q^2/2C$. Corresponding, respectively, to the magnetic loop and capacitor, $L\dot{Q}^2/2$ refers to the electrostatic energy stored in the ring, and $Q^2/2C$ refers to the energy in the slit. Accordingly, with an additional interaction term, the Lagrangian of the coupled MD system comprises a combination of the two individual SSRRs:

$$\Gamma = (L/2)(\dot{Q}_1^2 - \omega_0^2 Q_1^2) + (L/2)(\dot{Q}_2^2 - \omega_0^2 Q_2^2) + M\dot{Q}_1\dot{Q}_2.$$

Here, Q_1 and Q_2 are oscillatory charges in the respective SSRRs, M is the mutual inductance, and C is substituted with the relation $\omega_0=1/\sqrt{LC}$.

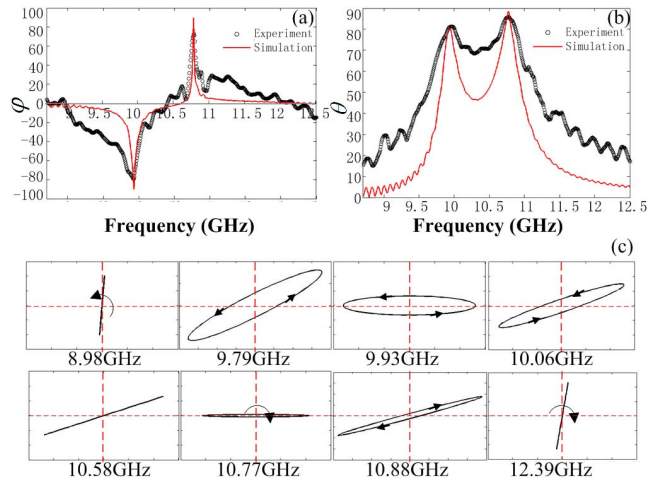


FIG. 3. (Color online) (a) Phase difference φ between x component and y component of transmitted wave: experimental result (black circle) and simulation result [gray (red) line]. (b) Rotation angle of the major polarization axis of transmitted wave (black circle; experiment results; red line: simulated results). (c) The change of polarization state on frequency with $D=1.56$ mm.

By solving the Euler–Lagrange equations, the eigenfrequencies $\omega_{\pm}=\omega_0/\sqrt{1\mp(M/L)}$ of the MP are obtained. These exhibit two magnetic resonant modes in this coupled system—the antibonding mode $|\omega_+\rangle$ that is characterized by an antisymmetric charge distribution ($Q_1=-Q_2$), and the bonding mode $|\omega_-\rangle$ that exhibits a symmetric charge distribution ($Q_1=Q_2$). Further, the frequency split of the two resonant modes $\Delta\omega=\omega_1-\omega_2\approx(M/L)\omega_0$ is changed by the strength of the coupling; thus, as the distance between the two SSRRs increases, the inductance M dramatically decreases, leading to a reduction in the frequency split $\Delta\omega$ [see Figs. 2(c) and 2(d)].

After studying the transmission property, we focus on the optical activity of this periodic array of MDs. For an observer facing the approaching wave, the profile of the E vector can be written as the following well-known equation:¹⁹

$$\left(\frac{E_x}{|E_x|}\right)^2 + \left(\frac{E_y}{|E_y|}\right)^2 - \frac{2E_x E_y}{|E_x||E_y|} \cos(\varphi_y - \varphi_x) = \sin^2(\varphi_y - \varphi_x).$$

We define the phase difference between the y and x components as $\varphi=\varphi_y-\varphi_x$. This determines the type of polarization state and the revolving direction: $\varphi=0$ indicates a linearly polarized state, while other conditions denote elliptical or circular polarization. Again, for an observer facing the approaching wave, the end point of the electric field revolves in the clockwise direction when $\sin\varphi>0$ and counterclockwise when $\sin\varphi<0$. We also employ the angle θ , defined as $\theta=\frac{1}{2}\arctan[2|E_x||E_y|\cos\varphi/(|E_x|^2-|E_y|^2)]$,¹⁹ that describes the angle between the major polarization axis and the y axis. This gives us a more intuitive picture about the changing of the elliptical polarization with frequency.

Figure 3 shows the experimental result of φ and θ when we set the distance between the SSRRs as 1.56 mm. From Fig. 3(a), we find that φ becomes zero at a frequency of 10.58 GHz, which divides the phase difference into two parts: negative and positive. Further, around the two resonant frequencies, φ reaches its extrema that are near -90° and 90° , respectively. At lower frequencies (<10.58 GHz),

sin $\varphi < 0$, the ellipse is counterclockwise, and the dimer constitutes an isomer of *d* type; at higher frequencies (> 10.58 GHz), sin $\varphi > 0$, the ellipse becomes clockwise and accordingly, the isomer is *l* type; and at exactly 10.58 GHz, the transmission briefly becomes linearly polarized. The rotation angle of the major polarization axes θ is shown in Fig. 3(b): as the frequency increases, the major polarization axis rotates quickly from the *y* axis and almost reaches the *x* axis at the resonant frequencies. Figure 3(c) presents a more intuitive description of the changing of the polarization state, wherein the curve made by the end point of the *E* vector is shown under eight specific frequencies. In the lower frequency region, the polarization of the transmission is a counterclockwise and compressed ellipse with the major axis slightly off the *y* axis. Then, the ellipse inflates and the major axis rotates toward the *x* axis. With the approach of the first resonant frequency, the ellipse shrinks again and becomes a flat ellipse with a 7° angle between the major axis and the *x* axis at a resonant frequency of 9.93 GHz. When the frequency reaches 10.58 GHz, the transmission becomes linearly polarized, and the ellipse begins to change its rotating direction to clockwise. Then, the ellipse compresses at the second resonant frequency of 10.77 GHz, where we observe that its major axis is almost along the *x* axis (with an angle of 2°). As the frequency increases, the major axis rotates forward to the *y* axis; the ellipse inflates at first but then deflates to a slender one almost horizontal to the *y* axis—similar to that at the low frequency. This indicates that at the resonant frequencies, the *y*-direction polarized incident wave becomes a very prolate elliptical wave with the major polarization axis near the *x* axis when passing through the array of MDs. Further, the area between the two resonance peaks exhibits transitional behaviors: there exist linear and various elliptical polarization states.

As discussed above, the slit of the first SSRR is along the *x* axis so that the incident wave generates a *y*-direction electric field in the slit; thus, this *y*-polarized incident wave is electrically coupled into the system. Through the strong magnetic interaction at the resonant frequency, energy is transferred from the first SSRR to the second one. As the electric field in the second slit is along the *x* axis, the electric dipole radiation generated in this slit gap is *x*-direction polarized. As a result, the transmission is a superposition of the *x*- and *y*-polarized states. At the two resonant frequencies, the interaction becomes extremely distinctive and the *x*-direction polarized wave reaches its maximum value in the transmission; thus, we obtain an elliptically polarized wave with the major axis almost along the *x* direction. Further, in the area far beyond the resonant frequency, a less *x*-direction polarized wave appears in the transmission so that the transmitted wave becomes a compressed ellipse near the *y* axis. As the distance between the SSRRs increases, the frequency gap shrinks and the two elliptical polarization states gradually join.

In this paper, we only realized the optical activity of MDs in the microwave range. Actually, the experimental verification of chiral metamaterials at optical frequencies is more interesting and should be realized in future studies.

In conclusion, we design a MD array comprising two SSRRs and experimentally investigate the behavior of the separated resonance peaks as well as their strong dependence on the distance between the two SSRRs. The optical activity of this periodic array of MDs caused by magnetic interaction is also studied in the transmission measurement; we found that a compressed, elliptically polarized transmitted wave can be achieved at the resonant frequency with the major polarization axes approximately perpendicular to that of the incident wave. Thus, these coupled SSRRs can function as a tunable optical activity medium, and this offers possible applications as a controllable polarizer.

This work was supported by the State Key Program for Basic Research of China (Nos. 2006CB921804 and 2004CB619003), the National Natural Science Foundation of China under Contract Nos. 10534042, 60578034, 10604029, and 10704036, and National Fundamental Fund of Personnel Training (No. J0630316).

- ¹J. B. Pendry, A. J. Holden, D. J. Robbins, and W. J. Stewart, *IEEE Trans. Microwave Theory Tech.* **47**, 2075 (1999).
- ²D. R. Smith, W. J. Padilla, D. C. Vier, S. C. Nemat-Nasser, and S. Schultz, *Phys. Rev. Lett.* **84**, 4184 (2000).
- ³R. A. Shelby, D. R. Smith, and S. Schultz, *Science* **292**, 77 (2001).
- ⁴R. Marqués, J. D. Baena, M. Beruete, F. Falcone, T. Lopetegui, M. Sorolla, F. Martín, and J. Garcia, *J. Opt. A, Pure Appl. Opt.* **7**, S38 (2005).
- ⁵T. J. Yen, W. J. Padilla, N. Fang, D. C. Vier, D. R. Smith, J. B. Pendry, D. N. Basov, and X. Zhang, *Science* **303**, 1494 (2004).
- ⁶S. Linden, C. Enkrich, M. Wegener, J. F. Zhou, T. Koschny, and C. M. Soukoulis, *Science* **306**, 1351 (2004).
- ⁷C. Enkrich, M. Wegener, S. Linden, S. Burger, L. Zschiedrich, F. Schmidt, J. F. Zhou, T. Koschny, and C. M. Soukoulis, *Phys. Rev. Lett.* **95**, 203901 (2005).
- ⁸V. M. Shalav, W. Cai, U. K. Chettiar, H. Yuan, A. K. Sarychev, V. P. Drachev, and A. V. Kildishev, *Opt. Lett.* **30**, 3356 (2005).
- ⁹N. Katsarakis, G. Konstantinidis, A. Kostopoulos, R. S. Penciu, T. F. Gundogdu, M. Kafesaki, E. N. Economou, T. Koschny, and C. M. Soukoulis, *Opt. Lett.* **30**, 1348 (2005).
- ¹⁰J. Zhou, Th. Koschny, M. Kafesaki, E. N. Economou, J. B. Pendry, and C. M. Soukoulis, *Phys. Rev. Lett.* **95**, 223902 (2005).
- ¹¹A. Ishikawa, T. Tanaka, and S. Kawata, *Phys. Rev. Lett.* **95**, 237401 (2005).
- ¹²H. Liu, D. A. Genov, D. M. Wu, Y. M. Liu, J. M. Steele, C. Sun, S. N. Zhu, and X. Zhang, *Phys. Rev. Lett.* **97**, 243902 (2006).
- ¹³J. B. Pendry, *Science* **306**, 1353 (2004).
- ¹⁴I. Tinoco and M. P. Freeman, *J. Phys. Chem.* **61**, 1196 (1957).
- ¹⁵A. Papakostas, A. Potts, D. M. Bagnall, S. L. Prosvirnin, H. J. Coles, and N. I. Zheludev, *Phys. Rev. Lett.* **90**, 107404 (2003).
- ¹⁶A. V. Rogacheva, V. A. Fedotov, A. S. Schwanecke, and N. I. Zheludev, *Phys. Rev. Lett.* **97**, 177401 (2006).
- ¹⁷J. M. Hao, Y. Yuan, L. X. Ran, T. Jiang, J. A. Kong, C. T. Chan, and L. Zhou, *Phys. Rev. Lett.* **99**, 063908 (2007).
- ¹⁸H. Liu, D. A. Genov, D. M. Wu, Y. M. Liu, Z. W. Liu, C. Sun, S. N. Zhu, and X. Zhang, *Phys. Rev. B* **76**, 073101 (2007).
- ¹⁹J. D. Jackson, *Classical Electrodynamics* (Wiley, New York, 1999).

CST 视频培训课程推荐

CST 微波工作室(CST Microwave Studio)是 CST 工作室套装中最核心的一个子软件,主要用于三维电磁问题的仿真分析,可计算任意结构任意材料电大宽带的电磁问题。广泛应用于高频/微波无源器件的仿真设计、各种类型的天线设计、雷达散射截面分析、电磁兼容分析和信号完整性分析等各个方面。

易迪拓培训(www.edatop.com)推出的 CST 微波工作室视频培训课程由经验丰富的专家授课,旨在帮助用户能够快速的学习掌握 CST 微波工作室的各项功能、使用操作和工程应用。购买 CST 教学视频培训课程套装,还可超值赠送 3 个月免费在线学习答疑,让您学习无忧。



CST 学习培训课程套装

该培训套装由易迪拓培训联合微波 EDA 网共同推出,是最全面、系统、专业的 CST 微波工作室培训课程套装,所有课程都由经验丰富的专家授课,视频教学,可以帮助您从零开始,全面系统地学习 CST 微波工作的各项功能及其在微波射频、天线设计等领域的设计应用。且购买该套装,还可超值赠送 3 个月免费学习答疑...

课程网址: <http://www.edatop.com/peixun/cst/24.html>

HFSS 天线设计培训课程套装

套装共含 5 门视频培训课程,课程从基础讲起,内容由浅入深,理论介绍和实际操作讲解相结合,全面系统的讲解了 CST 微波工作室天线设计的全过程。是国内最全面、最专业的 CST 天线设计课程,可以帮助您快速学习掌握如何使用 CST 设计天线,让天线设计不再难...

课程网址: <http://www.edatop.com/peixun/cst/127.html>



更多 CST 视频培训课程:

● CST 微波工作室入门与应用详解 — 中文视频教程

CST 微波工作室初学者的最佳培训课程,由工程经验丰富的资深专家授课,全程中文讲解,高清视频,直观易学。网址: <http://www.edatop.com/peixun/cst/25.html>

● CST 微波工作室天线设计详解 — 中文视频培训教程

重点讲解天线设计相关知识和使用 CST 进行天线仿真设计的使用操作,是学习掌握使用 CST 微波工作室进行天线设计的必备课程,网址: <http://www.edatop.com/peixun/cst/26.html>

● CST 阵列天线仿真设计实例详解 —— 中文视频教程

阵列天线设计专业性要求很高,因此相关培训课程是少之又少,该门培训课程由易迪拓培训重金聘请专家讲解;课程网址: <http://www.edatop.com/peixun/cst/123.html>

● 更多 CST 培训课程, 敬请浏览: <http://www.edatop.com/peixun/cst>

关于易迪拓培训:

易迪拓培训(www.edatop.com)由数名来自于研发第一线的资深工程师发起成立,一直致力和专注于微波、射频、天线设计研发人才的培养;后于 2006 年整合合并微波 EDA 网(www.mweda.com),现已发展成为国内最大的微波射频和天线设计人才培养基地,成功推出多套微波射频以及天线设计相关培训课程和 ADS、HFSS 等专业软件使用培训课程,广受客户好评;并先后与人民邮电出版社、电子工业出版社合作出版了多本专业图书,帮助数万名工程师提升了专业技术能力。客户遍布中兴通讯、研通高频、埃威航电、国人通信等多家国内知名公司,以及台湾工业技术研究院、永业科技、全一电子等多家台湾地区企业。

我们的课程优势:

- ※ 成立于 2004 年,10 多年丰富的行业经验
- ※ 一直专注于微波射频和天线设计工程师的培养,更了解该行业对人才的要求
- ※ 视频课程、既能达到现场培训的效果,又能免除您舟车劳顿的辛苦,学习工作两不误
- ※ 经验丰富的一线资深工程师讲授,结合实际工程案例,直观、实用、易学

联系我们:

- ※ 易迪拓培训官网: <http://www.edatop.com>
- ※ 微波 EDA 网: <http://www.mweda.com>
- ※ 官方淘宝店: <http://shop36920890.taobao.com>